JOURNAL OF CATALYSIS 109, 170–179 (1988)

The Adsorption of Oxygen and the Oxidation of Methanol on Silver–Platinum Alloys

DONG SHUZHONG,* XIAO FANHUA,† AND DENG JINGFA†,[1]

*Institute of Modern Physics and †Department of Chemistry, Fudan University, Shanghai, People's Republic of China

Received November 25, 1986; revised August 20, 1987

Ag–Pt alloy is prepared by hydrazine reduction in solution. The adsorption states of oxygen on Ag–Pt alloys containing Pt < 9.7 at.% are studied using XPS and TDS. The catalytic activity and selectivity of Ag–Pt alloys for oxidizing methanol into aldehyde are measured in a microreactor. Two kinds of adsorption states of oxygen are found on the surface of Ag–Pt alloy. It is shown that silver and platinum preserve their own characteristics of adsorbing oxygen after alloying. The Pt atoms alloyed with Ag promote the decomposition of formaldehyde. The rate equation of methanol oxidation on Ag–Pt alloy deduced on the assumption that the surface reaction is the rate-determining step fits the experimental results. © 1988 Academic Press, Inc.

INTRODUCTION

Silver as a catalyst is used for production of ethylene oxide from ethylene and aldehydes from alcohols (*1*). The adsorption of oxygen and the oxidation of methanol to formaldehyde on polycrystal or monocrystal silver have been studied intensively (*2, 3*). Three kinds of oxygen species, adsorbed atomic oxygen, adsorbed molecular oxygen, and subsurface atomic oxygen, have been observed on electrolytic silver at room temperature (*4*). Wachs and Madix (*5*) reported the reaction mechanism of methanol oxidation on Ag(110) single crystal with preadsorbed oxygen, and pointed out that the CH_3O was formed on the surface. This surface species was also found on electrolytic silver at room temperature and a different mechanism was postulated (*6*). The kinetics of methanol oxidation on silver was studied earlier. Bhattacharyya *et al.* (*7*) found fractional reaction orders for both methanol and oxygen at 290°C, and proposed an Eley–Rideal model for the reaction mechanism. Robb and Harriott (*8*) studied this reaction on a supported silver catalyst at 420°C. They assumed that oxygen is strongly adsorbed on silver, while methanol and the products are only adsorbed on top of the layer of adsorbed oxygen, and postulated a Langmuir–Hinshelwood model to fit their results.

The effects on the chemisorption and catalysis of metals by alloying are fascinating (*9*). We have found (*10*) that both electronic and catalytic properties of silver–palladium alloys vary with the alloy composition. And further, we have found that these two properties are interrelated. Platinum exhibits excellent characteristics for catalysis and is usually used for hydrogenation, dehydrogenation, isomerization, and so on (*11*). Yet it can also adsorb oxygen and has the catalytic capability to oxidize ammonia and carbon monoxide (*12–14*). Ag and Pd can be freely miscible, whereas Ag and Pt are not (*15*); i.e., Ag–Pt alloy possesses only limited solid solubility. The equilibrium phase diagram indicates that Ag and Pt form a binary peritectic system (*16*). The metastable solid solutions of Ag–Pt alloy over the whole concentration range can only be formed by rapidly quenching (*17*) but the alloys containing up to 10 at.% Pt and more than 94 at.% Pt can

[1] To whom correspondence should be addressed.

0021-9517/88 $3.00

be easily formed in a stable single phase (*18*). X-ray diffraction (XRD) are usually used as a characterization technique for Ag–Pt alloy (*15, 17, 18*). Ag–Pt alloy can be obtained by various methods (*18–21*). Among them, the chemical reduction from the solutions is rather suitable for catalysis research. The powder-form intermetallic compounds can be synthesized using the hydrazine reduction method in aqueous solutions (*22*). It has been shown that this method can also be used for the preparation of single-phase solid solutions, for example, Ag–Pd alloy (*10*), and now, Ag–Pt alloy. Studies on the catalytic property of Ag–Pt alloy are rare to date. Indzhikyan (*23*) showed that the catalytic activity of Pt for benzene hydrogenation dropped when it was alloyed with Ag. Recently, Wogelzang *et al.* (*24*) studied the selectivity of alloys in hydrocarbon reactions using Ag–Pt alloy as a model catalyst. DeJong *et al.* (*21, 25*) investigated the adsorption of nitrogen on silica-supported Pt–Ag alloy particles, and the results showed the extent of adsorption to drop strongly with the increasing silver content of the alloy. They all paid attention mainly to the effects of adding Ag to Pt.

The present work concerns the effects of alloying Ag with Pt on the adsorption and the oxidation of alcohol on Ag. The kinetics of alcohol oxidation on Ag–Pt alloys and the correlation between the surface and the catalytic properties of alloys are elucidated.

EXPERIMENTAL

1. The Preparation and Identification of Ag–Pt Alloys

Ag–Pt alloys with various compositions were prepared by the reduction of $Ag(NH_3)_4^+$ and $Pt(NH_3)_6^{+4}$ mixtures in aqueous solution with hydrazine hydrochloride. Metal ion–ammonia solution A and hydrazine–ammonia solution B were prepared, respectively. When solution A was added dropwise into solution B at 40°C with constant stirring, much gas was evolved and a dark gray powder precipitated. After the reaction ended, the precipitate was transferred to a filtering glass-sintering crucible, washed with distilled water and methanol, and then dried at 120°C. The average size of the precipitate particles was determined by scanning electron microscopy (SEM). The XRD patterns were obtained using a "Rigaku" D/Max-rB diffractometer equipped with Cu$K\alpha$ radiation filtered through a graphite monochromator. The diffractometer settings were the following: X-ray tube current, 100 mA; X-ray tube potential, 40 kV; divergence slit, 1°; receiving slit, 0.15 mm; monochromator receiving slit, 0.6 mm; scanning rate, 4°/min; time constant, 0.5 sec. According to the results of chemical analysis, the Ag–Pt alloys obtained contained 1.1, 5.1, 6.8, 9.7, and 94.7 at.% Pt, respectively.

2. The Measurements of the Catalytic Activity of Alloys Concerning Methanol Oxidation

The catalytic activities of Ag–Pt alloys for methanol oxidation were determined with a continuous microreactor. The reactor, a stainless-steel tube with an i.d. of 0.5 cm, was loaded with 0.5 g catalyst. The temperature of the catalyst was measured with a Ni–Cr/Ni–Al thermocouple. The catalysts were activated at 500°C for 4 hr in H_2 flow at first, and then N_2 instead of H_2 was passed through the reactor for 1 hr. Methanol was injected into an evaporator by a micropump in order to be mixed with air before entering the reactor. The temperature of the catalyst was then controlled at 300 ± 0.5°C. The mole ratio of oxygen to methanol was 0.4. Space velocity was 3.64×10^4 hr^{-1}. The products passed through a bypass valve and entered the first gas chromatograph with a porapak-N column so that the quantities of aldehyde, methanol, and H_2O could be determined, and then they passed through another bypass valve and entered the second gas chromatograph with a TDX-01 column so that the contents of H_2, CO, CO_2, and O_2 residue could be determined. The quantity of the tail gas was

measured by a flow meter. The response factors of the peak areas of HCHO, CH_3OH, and H_2O for the porapak-N column were 1.00, 0.45, and 0.23 and those of H_2, air, CO, and CO_2 for the TDX-01 column were 51.7, 1.00, 0.96, and 0.8, respectively. The separation efficiency of these gases in the corresponding columns described above were excellent.

3. *The Determination of the Kinetic Equation for Methanol Oxidation with Differential Reactor*

The methanol and pure oxygen (99.99%) as well as the carrier gas nitrogen were mixed and entered into the reactor at a flow of 370 ml/min. The conversion of methanol was controlled at about 5%. Ag–Pt alloy (0.5 g) containing 9.7 at.% Pt was mixed with quartz sand in the ratio of catalyst to sand of 1 : 20 in order to reduce the effect of reaction heat. The catalyst was loaded into the reactor and was activated at 500°C. After the activation, the temperature of the catalyst was reduced to 350°C and then the catalytic activity was measured. The analytical methods of the products and the calculation of the reaction rate were the same as those described in the literature (*26, 27*). The diffusion effects were negligible in our experiment. During the reaction, only HCHO and CO_2 could be detected; no CO or other by-products were found.

4. *XPS Experiment*

The composition of the alloy surface and the adsorption of oxygen on Ag–Pt alloys were studied by using XPS in a VG ESCALAB 5 electron spectrometer as described in (*4*). The X-ray source used was Mg$K\alpha$. The testing chamber of the electron spectrometer maintained vacuum pressure on the order of 10^{-8} Pa during the experiments. The sample used was a disk of ϕ 10 × 1 mm obtained from the alloy powder by a press. The sample surface was cleaned by argon ion bombardment and oxidation (P_{O_2} of 10^{-4} Pa)–annealing (600°C) cycles in the sample preparation chamber of the electron spectrometer with a background pressure on the order of 10^{-8} Pa until the signals of C and O were diminished to the noise level. Oxygen was introduced into the chamber through a variable UHV leak valve. The binding energy measurements were calibrated by using E_B (Ag $3d_{5/2}$) = 368.0 eV. The surface compositions of the alloys were calculated with the peak area of their XPS according to the relative sensitivity factors of the elements (*28*). Here the surface composition means the atom composition of a zone probed by XPS, which usually only has a few atom layers near the surface dependent on the escape length of the photoelectrons and the instrument geometry.

5. *Thermal Desorption of Oxygen Adsorbed on Alloy Containing 9.7 at.% Pt*

The experiment was done in a UHV chamber equipped with a quadrupole mass spectrometer. Pumping was accomplished with a titanium sputter ion pump (300 liter/sec). The background pressure of the chamber was on the order of 10^{-6} Pa. The alloy powder was placed in a quartz tube connected directly to the chamber. The sample was heated by a conventional electric heater around the sample outside the tube. The heating rate β for desorption was 2.5 K/sec. A variable leak valve was used for introducing oxygen. The exposure pressure of oxygen was 5×10^{-4} Pa. The result of the empty test of quartz tube as a background was subtracted from the desorption results of the samples. At the initial stage of the desorption experiments, only a small amount of oxygen desorbed, but the TDS of CO (M = 28) could be obtained. The alloy powder was treated by the adsorption–desorption (to 700°C) cycle repeatedly until no TDS of CO could be observed and the TDS of O_2 could be repeated. Then the sample adsorbed with oxygen was heated linearly with time from room temperature to 700°C and the TDS of O_2 was recorded.

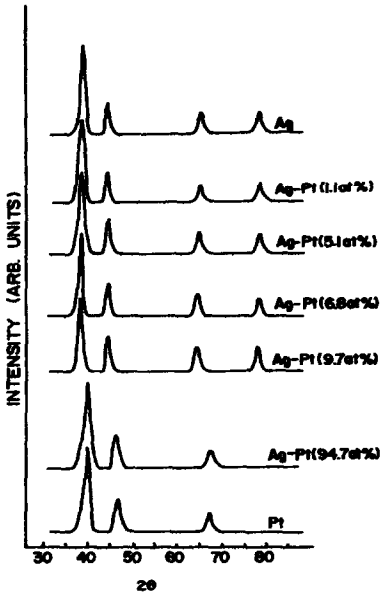

FIG. 1. X-ray diffraction spectra of Ag–Pt alloy.

RESULTS AND DISCUSSIONS

1. The Homogeneity of the Samples

The results of the X-ray diffraction of the alloys obtained are presented in Fig. 1 and show that the X-ray diffraction lines of the alloys were similar to those of pure silver or pure platinum, indicating a platinum content of the alloys less than 9.7 at.% or more than 94.7 at.%, respectively. No free Pt could be detectable as the bulk compositions of the alloys were <9.7 at.% Pt. The Pt contents of the samples used are clearly high enough to be detected; this is true in the case of two samples of 5.1 and 9.7 at.% Pt at least. Further increasing the Pt content in the alloy of 9.7 at.% Pt, the second phase, free Pt or a diluted solid solution rich in Pt, was detected by XRD. The miscible ranges obtained are also consistent with those in the literature (*18*). The results indicate that Pt should be alloyed with Ag in the samples. The size of the alloy particles obtained was about 1 μm or less, observed by SEM. The samples were treated by annealing or an oxidation-annealing cycle at 600°C repeatedly before being tested in the experiment; as a result the samples should be homogeneous in composition even if the raw precipitate had some inhomogeneity.

The XPS results show that the surface compositions of Ag–Pt alloys are affected by the pretreatment of the samples and usually deviate from their bulk values. After annealing at about 600°C, the alloy surface is rich in silver, but it can be changed to be platinum-rich by argon ion bombardment due to preferential sputtering. Two samples used for XPS studies of oxygen adsorption contain 5.1 and 9.7 at.% Pt in bulk, but their Pt concentrations obtained from XPS are 2.2 ± 0.2 and 4.2 ± 0.3 at.%, respectively, after cleaning cycle treatments. We did not find any change of the surface composition when the samples were exposed to oxygen. It indicated that the adsorption of oxygen did not induce observable change of the surface composition of Ag–Pt alloys in our experiments. The surface composition of the alloy still did not change after being used as catalyst, although the C content on the surface increased.

2. The Adsorption of Oxygen on Ag–Pt Alloys

The XPS spectra of oxygen on alloys at various exposures are shown in Fig. 2. For alloy containing 5.1 at.% Pt (Fig. 2a), a

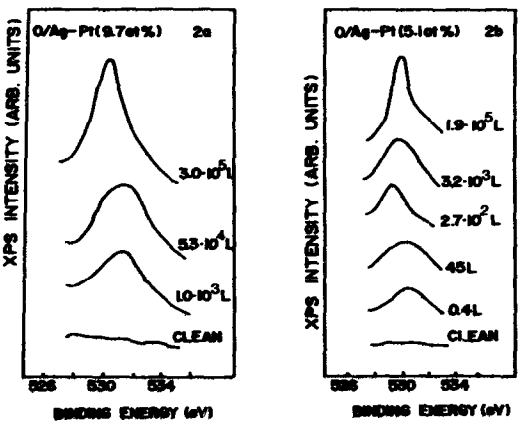

FIG. 2. O 1*s* spectra of XPS on Ag–Pt alloy.

weak peak of O 1*s* appeared at about 531 eV at low exposures (0.4 L), another peak at 529.6 eV appeared when the exposure was increased, and finally, when the exposure further increased ($>10^3$ L) a peak at 530.2 eV was formed. For Ag–Pt alloy containing 9.7 at.% Pt (Fig. 2b), the XPS of O 1*s* was similar to that of alloy containing 5.1 at.% Pt except that the peak at 531 eV was observable even at larger exposures (10^4 L) and at 529.6 eV no peak appeared. The XPS difference spectra of O 1*s* (Fig. 3) show that there are two differences between Ag and Ag–Pt alloys. First, an adsorption state of atomic oxygen with E_B = 529.6 eV existed on both Ag and Ag–Pt alloy containing 5.7 at.% Pt, but it has not been found on Ag–Pt alloy containing 9.7 at.% Pt. The atomic adsorption state of oxygen with E_B = 530.2 eV was the major part of the oxygen species at large exposures on all three surfaces. Second, no peak of E_B (O 1*s*) = 531 eV has been detected on pure silver, but it has been observed on both Ag–Pt alloy surfaces. The amount of this oxygen species adsorbed on Ag–Pt alloy containing 9.7 at.% Pt is larger than that on the alloy containing 5.1 at.% Pt under similar experimental conditions. We had studied the adsorption of oxygen on electrolytic silver (*4*) and indicated that the adsorption state of oxygen for which E_B (O 1*s*) = 529.6 eV was connected with some defects of the silver surface, and the oxygen species corresponding to an E_B of 530.2 eV pertains to surface and subsurface atomic oxygen. Because of the fact that the peak of O 1*s* at 531 eV only appeared on Ag–Pt alloy surfaces, we determined that the corresponding adsorption state of oxygen resulted from the interaction between the oxygen atom and the surface site related to the Pt atom. Platinum is stronger in adsorbing oxygen atoms (*29*). Oxygen may be adsorbed preferentially on the surface site related to the Pt atom; hence the peak of 531 eV appears first when the alloy sample is exposed to oxygen. The population of the site related to the Pt atom on the surface should be far less than that of Ag owing to the low concentration of Pt, so the major parts of the oxygen species adsorbed on both Ag–Pt and Ag at large exposures are identical. But a small amount of Pt atoms may be enough to affect the defect on surface. When the Pt contents of alloys changed from 5.1 to 9.7 at.%, the peak of E_B = 529.6 eV disappeared and the peak of E_B = 531 eV heightened. This suggests that the related defect site may be occupied by a Pt atom.

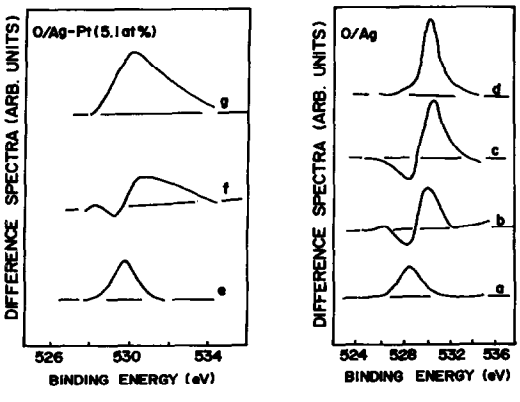

FIG. 3. O 1*s* difference spectra for different exposures (in L) of oxygen adsorbed on electrolytic silver and Ag–Pt (5.7 at.%) alloy: (a) 4×10^3 to 2×10^2; (b) 1.1×10^5 to 4×10^3; (c) 1.4×10^6 to 1.1×10^5; (d) 1.7×10^9 to 1.4×10^6; (e) 2.7×10^2 to 45; (f) 3.2×10^3 to 2.7×10^2; (g) 1.9×10^5 to 3.2×10^3.

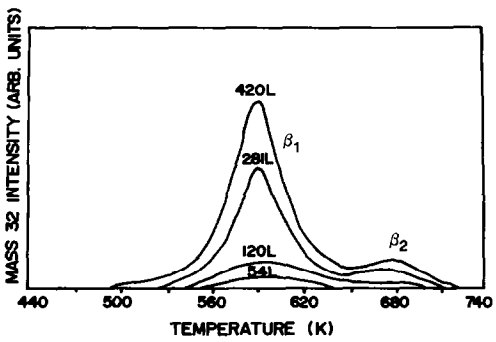

FIG. 4. TDS of oxygen adsorbed on Ag–Pt (9.7 at.%) alloy at room temperature, β = 2.5 Ksec^{-1}.

The TDS of oxygen adsorbed on Ag–Pt alloy containing 9.7 at.% Pt are presented in Fig. 4 and show that two different ad-

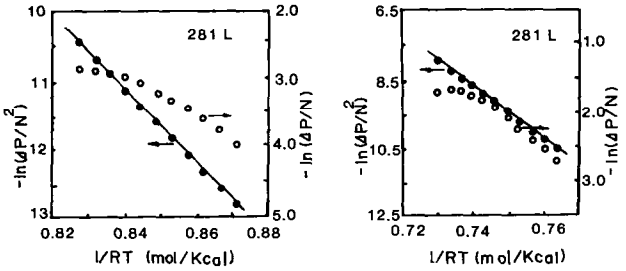

FIG. 5. Plots of $\ln(\Delta P/N^n)$ versus $1/RT$ from TDS: (a) peak β_1; (b) peak β_2.

sorption states of oxygen coexist on an alloy surface at room temperature. The TDS peaks β_1 and β_2 corresponding to two adsorption states of oxygen were observed at T_p of 580 ± 10 and about 660 K, respectively. The shapes of both peaks are symmetric. The activation energies of desorption E_d can be estimated with the equation (*30*)

$$-\frac{d\ln(\Delta P/N^n)}{d(1/T)} = E_d/R,$$

where ΔP is the intensity of the mass spectroscopic peak for M32, N is the oxygen atom number adsorbed on an alloy surface (atoms/cm), n is the desorption order, and T is the desorption temperature. Both peaks exhibit the characteristics of second-order desorption as shown in Fig. 5. The E_d values obtained from the TDS of oxygen with different exposures are listed in Table 1.

The peak β_1 results from the desorption of the atomic adsorption state of oxygen on Ag although its E_d is slightly higher (*4*), but peak β_2 has not been found for Ag. Much of the literature (*12, 31, 32*) showed that there were multiplets for the thermal desorption of oxygen on poly- or monocrystal Pt, and that peaks similar to β_2 appeared for Pt (*31, 32*). This suggested that β_1 and β_2 peaks of TDS obtained from Ag–Pt alloy correlated to the adsorption states on the sites related to Ag and Pt atoms, respectively. This TDS result is consistent with that from the XPS. We consider that the neighbor bridge or hollow positions about a single Pt atom may be the main adsorption sites related to the Pt atom. The adsorption sites which neighbor with two or more Pt atoms are negligible due to their scarce population. Here, that using a complete crystal plane to describe the adsorption surface is unsuitable. The surface of the alloy powder formed from the chemical reduction in the solution is different from the smooth flat surface of various single crystals and films. It is obvious that there are various defects on the surface of the alloy particles. They should play an important role in adsorbing oxygen especially at low coverages. This may be the reason that the desorption energy of oxygen on samples presented a higher value.

3. Correlation between the Catalytic Activity and the Surface Property of Ag–Pt Alloys

The catalytic activities for methanol oxidation on Ag–Pt alloys obtained at 300°C and a ratio of oxygen to alcohol of 0.4 are given in Fig. 6 and show that the conver-

TABLE 1

Activation Energies of Oxygen Desorption from Ag–Pt (9.7 at.%) Alloy

Exposure (L)	E_d (kcal/mole)	
	From β_1	From β_2
281	55.2	79.6
420	52.1	83.4
548	51.1	102.1

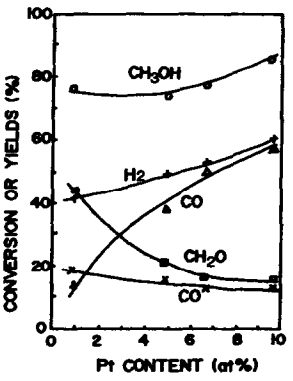

FIG. 6. Methanol conversion and product yields for methanol oxidation on Ag–Pt alloy.

sion of methanol X_m increased slightly with the increment of the Pt content of the alloys, and at the same time, the yields and selectivities of formaldehyde decreased rapidly until the Pt content of alloys neared 7 at.%, and then they remained unchanged. The yields of H_2 and CO also increase with the increasing Pt content of alloys and the yield ratio of H_2 to CO was approximated to 1 as the Pt content of alloy was more than 7 at.%. We have found that there is a correlation between the increase in CO yield and the decrease in formaldehyde yield. This suggests that CO results from the decomposition of formaldehyde. The inference has been verified by the experiment of catalytic decomposition of formaldehyde on Ag–Pt alloys.

The binding energies of core level Ag $3d_{5/2}$ and Pt $4f_{7/2}$ shifted a little when Pt content increased in Ag–Pt alloy as shown in Table 2. The decreases in the binding energies with the increases in the Pt contents of alloys indicate that the electron densities around Ag atoms are increased, which is advantageous to the provision of the electron to the oxygen atom from silver and to the formation of the atomic adsorption state of oxygen on the surface. The result is the fact that the conversion of methanol slightly increased with the increase in the Pt content of alloys. The reaction between methanol and oxygen atom adsorbed on Ag is dependent on the strength of the adsorption of oxygen on the surface (*6*). If the adsorption of oxygen is too weak, the conversion of methanol would be low, but strong adsorption will result in a decrease in the selectivity. Both results of XPS and TDS showed that a stronger adsorption state of oxygen corresponding to the interaction between the oxygen atom and the adsorption sites related to the Pt atom on surface existed, which resulted in the decomposition of formaldehyde, and then the yield of formaldehyde as well as selectivity dropped and the yields of CO and H_2 rose. The results from the methanol oxidation on Ag–Pt alloys were consistent with those on Ag–Pd alloys (*10*).

4. The Kinetics of Methanol Oxidation on Alloys

It was indicated that both methanol and formaldehyde could not be adsorbed on clean silver, but that induced adsorption and reaction of methanol could occur on the surface with oxygen preadsorbed (*6*). It has been shown that the majority of oxygen was adsorbed on Ag–Pt alloys to form an atomic adsorption state similar to that on silver. Therefore, we can propose a mechanism of methanol oxidation on Ag–Pt alloys similarly to what Robb and Harriott (*8*) did on a supported Ag catalyst. The kinetic model postulated is

TABLE 2

Binding Energies E_B of Ag $3d_{5/2}$ and Pt $4f_{7/2}$

Pt content of alloy (at.%)	E_B (eV)	
	Ag $3d_{5/2}$	Pt $4f_{7/2}$
0	367.9	—
1.1	367.9	69.9
5.1	367.8	69.9
9.7	367.7	70.1
94.7	367.1	70.6
100	—	70.6

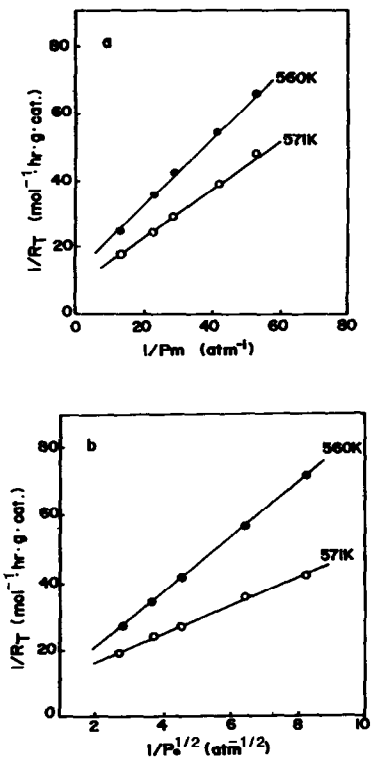

FIG. 7. (a) Plots of $1/R_T$ versus $1/P_m$, when P_o = constant; (b) plots of $1/R_T$ versus $1/P_o^{1/2}$, when P_m = constant.

$$O_2 + 2S \underset{k_{-1}}{\overset{k_1}{\rightleftharpoons}} 2O\text{–}S \qquad (1)$$

$$M + O\text{–}S \underset{k_{-2}}{\overset{k_2}{\rightleftharpoons}} M\text{–}O\text{–}S \qquad (2)$$

$$M\text{–}O\text{–}S \xrightarrow{k_3} P + S \qquad (3)$$

$$P + O\text{–}S \underset{k_{-4}}{\overset{k_4}{\rightleftharpoons}} P\text{–}O\text{–}S \qquad (4)$$

If the surface reaction (step 3) is the rate-determining step, and the adsorptions of methanol and the products do not affect the adsorption equilibrium of oxygen, then the rate formula deduced is

$$R_T = \frac{k_3 K_o^{1/2} K_m P_o^{1/2} P_m}{(1 + K_m P_m + K_p P_p)(1 + K_o^{1/2} P_o^{1/2})}, \qquad (1)$$

where $K_o = k_1/k_{-1}$, $K_m = k_2/k_{-2}$, $K_p = k_4/k_{-4}$; P_o, P_m, and P_p are the pressures of oxygen, methanol, and products, respectively.

In order to check the rate formula, the kinetic test can be done with a differential reactor. In such experiments, the conversion of methanol was low (5%) and only a small amount of the product was formed, so the term $K_p P_p$ can be neglected in formula (1), and the rate formula can be simplified,

$$R_T = \frac{k_3 K_m P_m K_o^{1/2} P_o^{1/2}}{(1 + K_m P_m)(1 + K_o^{1/2} P_o^{1/2})}. \qquad (2)$$

The formula (2) can be transformed into

$$1/R_T = \frac{1 + K_m P_m}{k_3 K_m P_m K_o^{1/2}} \cdot \frac{1}{P_o^{1/2}} + \frac{1 + K_m P_m}{k_3 K_m P_m} \qquad (3a)$$

and

$$1/R_T = \frac{1 + K_o^{1/2} P_o^{1/2}}{k_3 K_o^{1/2} P_o^{1/2} K_m} \cdot \frac{1}{P_m} + \frac{1 + K_o^{1/2} P_o^{1/2}}{k_3 K_o^{1/2} P_o^{1/2}}. \qquad (3b)$$

Figures 7a and 7b obtained from the experimental data show that the reciprocal of the reaction rate $1/R_T$ is proportional to the reciprocal of the methanol pressure $1/P_m$ when oxygen pressure P_o is constant; $1/R_T$ is proportional to the $1/P_o^{1/2}$ when $1/P_m$ is constant. It is consistent with the results predicted by the rate equation (3a), (3b) deduced above. The kinetic parameters calculated from Fig. 7 are listed in Table 3. We fit the values k_3, K_m, and K_o into formula (3), calculate the reaction rate at varying oxy-

TABLE 3

Kinetic Parameters Calculated from Fig. 7

T (K)	k_3 (mol · hr^{-1} · g cat^{-1})	K_m (atm^{-1})	K_o (atm^{-1})	$k_3 K_m K_o^{1/2}$ (mol · hr^{-1} · g cat^{-1} · atm$^{-3/2}$)
560	1.2	8.27	0.084	2.87
571	0.43	12.4	1.23	5.92

TABLE 4

Comparison between the Calculated Kinetic Rate and Their Experimental Values

T (K)	$P_m \times 10^2$ (atm)	$P_o \times 10^2$ (atm)	$R_T \times 10^2$ (mol · hr^{-1} · g cat^{-1})	
			Experimental	Calculated
560	6.71	1.46	1.44	1.45
	6.71	2.31	1.81	1.80
	6.71	4.53	2.38	2.48
	6.71	6.75	2.94	2.99
	6.71	11.20	3.91	3.78
571	1.87	11.35	2.14	2.14
	2.52	11.35	2.63	2.71
	3.64	11.35	3.56	3.54
	4.67	11.35	4.21	4.18
	7.14	11.35	5.26	5.34

gen and methanol pressures, and then compare the calculated results with the experimental values (Table 4).

The calculated reaction rate is consistent with the experimental results, which indicates that the assumed chemical kinetic model is reasonable under our experimental conditions. The results show that the amount of Pt atoms on the surface of Ag–Pt alloy is so small that the kinetics of methanol oxidation on unsupported Ag–Pt alloy containing <9.7 at.% Pt is identical with that on supported Ag catalyst.

CONCLUSIONS

1. A homogeneous solid solution of Ag–Pt in the Pt content range of <9.7 at.% or >94.7 at.% can be prepared by chemical reduction in the solution.

2. Two kinds of the atomic adsorption states of oxygen exist on the surface of Ag–Pt alloy. One is similar to that on pure silver; the other is related to Pt atom alloyed with Ag. The strength of O–Ag and O–Pt chemisorption bonds does not vary obviously when alloyed.

3. The sites related to Pt atom on the surface of Ag–Pt alloy can promote the decomposition of formaldehyde and then decrease the yields and selectivities for formaldehyde.

4. The kinetics of the methanol oxidation on Ag–Pt alloy containing <9.7 at.% Pt can be described by a model as that on Ag on the assumption that the surface reaction transforming the surface species into the products is the rate-determining step.

ACKNOWLEDGMENT

We are grateful to the National Science Foundation of China for their support of this work.

REFERENCES

1. Kilty, P. A., and Sachtler, W. M. H., *Catal. Rev.* **10,** 1 (1974).
2. Czanderna, A. W., *J. Phys. Chem.* **68,** 2765 (1964).
3. Barteau, M. A., and Madix, R. J., *in* "The Chemical Physics of Solid Surface and Heterogeneous Catalysis" (D. A. King and D. P. Woodruff, Eds.), Vol. 4, p. 100. Elsevier, Amsterdam, 1982.
4. Bao, X. H., Deng., J. F., and Dong, S. Z., *Surf. Sci.* **163,** 444 (1985).
5. Wachs, I. E., and Madix, R. J., *Surf. Sci.* **76,** 531 (1978).
6. Bao, X. H., and Deng, J. F., *J. Catal.* **99,** 391 (1981).
7. Bhattacharyya, S. K., Nag, N. K., and Ganguly, N. D., *J. Catal.* **23,** 158 (1971).
8. Robb, D. A., and Harriott, P., *J. Catal.* **35,** 176 (1974).
9. Ponec, V., *in* "The Chemical Physics of Solid Surface and Heterogeneous Catalysis" (D. A. King and D. P. Woodruff, Eds.), Vol. 4, p. 365. Elsevier, Amsterdam, 1982.
10. Deng, J. F., Zhu, X. Z., Dong, S. Z., and Pang, Y. W., *Acta Chim. Sin.* **42,** 1133 (1984). [China]
11. Somorjai, G. A., "Chemistry in Two Dimensions: Surface." Cornell Univ. Press, Ithaca, 1981.
12. Gland, J. L., Sexton, B. A., and Fisher, G. B., *Surf. Sci.* **95,** 587 (1980).
13. Barteau, M. A., Ko, E. I., and Madix, R. J., *Surf. Sci.* **104,** 161 (1981).
14. Gland, J. L., and Korchak, V. N., *J. Catal.* **53,** 9 (1978).
15. Hume-Rothery, W., *Platinum Met. Rev.* **10,** 94 (1966).
16. Klement, W., Jr., and Luo, H. L., *Trans. Metall. Soc. AIME* **227,** 1253 (1963).
17. Duwez, P., *in* "Techniques of Metals Research I" (R. F. Bunshah, Ed.). Wiley–Interscience, New York, 1968.
18. Ebert, H., *J. Less-Common Met.* **91,** 89 (1983).
19. Hideaki, K., *J. Phys. Soc. Japan* **43,** 711 (1977).
20. Hirsch, H., *Nature (London)* **213,** 793 (1967).
21. DeJong, K. P. Bongenaar-Schlenter, B. E., Meima, G. R., Verkerk, R. C., Lammers, M. J. J., and Geus, J. W., *J. Catal.* **81,** 67 (1983).

22. Kulifay, S. M., *J. Amer. Chem. Soc.* **83,** 4916 (1961).
23. Indzhikyan, M. A., *Arm. Khim. Zh.* **20,** 349 (1967).
24. Wogelzang, M. W., Botman, M. J. P., and Ponec, V., *Faraday Discuss. Chem. Soc.* **72,** 33 (1981).
25. DeJong, K. P., Meima, C. R., and Geus, J. W., *Appl. Surf. Sci.* **14,** 73 (1982/83).
26. Deng, J. F., and Zhu, X. Z., *J. Catal.* **4,** 266 (1983). [China]
27. Bhattacharyya, S. K., *J. Catal.* **8,** 128 (1967).
28. Mingren, Y., Yanwan, P., and Xun, W., *J. Appl. Sci.* **2,** 140 (1984). [China]
29. Toyoshima, I., and Somorjai, G. A., *Catal. Rev.* **19,** 105 (1979).
30. Menzel, D., *in* "Interactions on Metal Surfaces" (R. Gomer, Ed.), p. 102. Springer-Verlag, Berlin, 1975.
31. Alnot, M., Fusy, J., and Cassuto, A., *Surf. Sci.* **72,** 467 (1978).
32. Norton, R. R., Griffiths, K., and Binduer, P. E., *Surf. Sci.* **138,** 125 (1984).